JVI Accepts, published online ahead of print on 30 April 2014
J. Virol. doi:10.1128/JVI.00912-14

Exceptionally potent neutralization of MERS-CoV by human monoclonal antibodies

Tianlei Ying,[a]# Lanying Du,[b] Tina W. Ju,[a] Ponraj Prabakaran,[a] Candy C. Y. Lau,[c] Lu Lu,[d] Qi Liu,[d] Lili Wang,[b] Yang Feng,[a] Yanping Wang,[a] Bo-Jian Zheng,[c] Kwok-Yung Yuen,[c] Shibo Jiang,[b,d] and Dimiter S. Dimitrov[a]#

Protein Interactions Group, Laboratory of Experimental Immunology, Cancer and Inflammation Program, Center for Cancer Research, National Cancer Institute, National Institutes of Health, Frederick, Maryland, USA[a]; Lindsley F. Kimball Research Institute, New York Blood Center, New York, New York, USA[b]; Department of Microbiology, University of Hong Kong, Pokfulam, Hong Kong[c]; Key Laboratory of Medical Molecular Virology of Ministries of Education and Health, Shanghai Medical College and Institute of Medical Microbiology, Fudan University, Shanghai, China[d]

Running Head: human mAbs against MERS-CoV

#Address correspondence:

Tianlei Ying, yingt@mail.nih.gov; Dimiter S. Dimitrov, dimiter.dimitrov@nih.gov

Key words: therapeutic antibodies, coronaviruses, MERS-CoV

Word Count for the Abstract: 249.

Word Count for the text: 4993

ABSTRACT

The recently discovered Middle East Respiratory Syndrome Coronavirus (MERS-CoV) continues to infect humans with high mortality. Specific, highly effective therapeutics and vaccines against the MERS-CoV are urgently needed to save human lives and address the pandemic concerns. We identified three human monoclonal antibodies (mAbs), m336, m337 and m338, targeting the receptor (CD26/DPP4) binding domain (RBD) of the MERS-CoV spike glycoprotein from a very large naive antibody library (size ~ 10^{11}). They bound with high affinity – equilibrium dissociation constants equal to 4.2, 9.3 and 15 nM, respectively, as measured by Biacore for Fabs binding to RBD. The avidity for IgG1 m336, m337 and m338 was even higher – 99, 820 and 560 pM, respectively. The antibodies bound to overlapping epitopes which overlap with the receptor binding site on the RBD as suggested by competition experiments and further supported by site-directed mutagenesis of the RBD and a docking model of the m336-RBD complex. The highest affinity mAb, m336, neutralized both pseudotyped and live MERS-CoV with exceptional potency: 50% neutralization at 0.005 and 0.07 μg/ml, respectively, likely by competing with DPP4 for binding to the S glycoprotein. The exceptionally high neutralization activity of these antibodies and especially m336 suggests that they have great potential for prophylaxis and therapy of MERS-CoV infection in humans and as a tool for development of vaccine immunogens. The rapid (several weeks) identification of potent mAbs suggests a possibility to use the new large antibody library and related methodology for quick response to public threat resulting from emerging coronaviruses.

48 **IMPORTANCE**

49 A novel human coronavirus, the Middle East Respiratory Syndrome Coronavirus (MERS-CoV)
50 was found to infect humans with a high mortality rate in 2012, just a decade after the appearance
51 of the first highly pathogenic coronavirus, SARS-CoV. There are no effective therapeutics
52 available. It is highly desirable to find an approach for rapidly developing potent therapeutics
53 against MERS-CoV, which can not only be implemented for MERS treatment, but can also help
54 to develop a platform strategy to combat future emerging coronaviruses. We report here the
55 identification of human monoclonal antibodies (mAbs) from a large non-immunized antibody
56 library that target the MERS-CoV. One of the antibodies, m336, neutralized the virus with
57 exceptional potency. It therefore may have great potential as a candidate therapeutic and as a
58 reagent to facilitate the development of vaccines against MERS-CoV.
59
60
61
62
63
64
65
66
67
68
69
70

INTRODUCTION

In September 2012, a novel human coronavirus, the Middle East Respiratory Syndrome Coronavirus (MERS-CoV), was isolated from a Saudi Arabian patient suffering from severe pneumonia who later died of respiratory and renal failure (1). Following that, a cluster of 23 laboratory-confirmed cases of MERS-CoV infections were identified between April 1 and May 23, 2301 and investigated including full-genome sequencing of MERS-CoV from four patients (2). As of March 27, 2014, 206 infections, including 86 deaths, had been reported (http://www.who.int/csr/don/2014_03_27_mers). Although past outbreaks have been contained, more clusters and sporadic cases have originated from multiple sources, indicating a natural animal reservoir and the potential for future outbreaks (3-5). It is also notable that the clinical, epidemiological, and virological features of MERS-CoV are similar to that of the severe acute respiratory syndrome coronavirus (SARS-CoV), which is the first highly pathogenic coronavirus appeared about a decade ago and caused a global pandemic with more than 800 deaths worldwide within a few months. A number of new coronaviruses have been identified since the outbreak of SARS, and accumulating evidences indicate that coronaviruses are able to rapidly and stably adapt to new host species (6). These findings indicate that SARS-CoV and MERS-CoV-like novel coronaviruses are highly likely to continue to emerge and pose a serious threat to human health in the near future.

There are currently no effective therapies against MERS-CoV. Recently, a study reported that rhesus macaques treated with IFN-α2b and ribavirin, which does not directly target the virus but reduces damaging inflammation of the lung, exhibited reduced MERS-CoV replication and an improved clinical outcome (7). However, the treatment was initiated soon (8 hours) after challenge and the disease in the macaques was at best mild to moderate in severity, so whether

the drug cocktail would work when faced with severe human disease, which may take longer to develop, remains unclear. Broad-spectrum antivirals have not proven to be effective in the clinic, and in fact there are currently no approved antiviral treatments for any human coronavirus infections. Thus, it is urgent to find an approach to rapidly develop potent therapeutics against MERS-CoV, which can not only be implemented for the treatment of MERS, but can also help to develop a platform strategy against emerging coronaviruses in the future.

Monoclonal antibodies (mAbs) are enjoying significant success in the clinic and have been used for the effective treatment of a number of diseases, in particular, cancer and immune disorders (8-11). Although more than 40 mAbs have been approved for clinical use, the humanized mAb Synagis (palivizumab) (12) remains the only mAb approved by the FDA for use against a viral disease. However, an increasing number of mAbs against emerging viruses, as well as against HIV-1 and other viruses, have been developed. Some of these mAbs are promising candidate therapeutics and some were used on compassionate basis for prophylaxis of humans exposed to virus (13-15).

We previously developed an mAb, m102.4 against the emerging viruses Hendra (HeV) and Nipah (NiV) which was administered on a compassionate basis to humans exposed to HeV based on its efficacy *in vitro* and in animals (16-19). We have also discovered mAbs against SARS-CoV which exhibited potent neutralization of SARS-CoV isolates (20). In this study, we constructed a novel very large (size ~ 10^{11}) IgM library by using B cells from the blood of 40 healthy donors in order to enhance selection of high-affinity antibodies with minimal divergence from their germline predecessors, and engineered a fragment containing the MERS-CoV S protein receptor binding domain (RBD), which is a major MERS-CoV neutralization determinant. This RBD was used as a selecting antigen for panning of the library. A panel of

antibodies were identified and characterized. Here we present evidence that three of these antibodies have exceptionally potent neutralization activity against MERS-CoV. These antibodies could be useful for prophylaxis of MERS and treatment of MERS-CoV infected patients and as reagents to facilitate development of therapeutics and vaccines as well as to help understand their mechanisms of action.

MATERIALS AND METHODS

Generation, Expression and Characterization of MERS-CoV RBD, RBD Mutants and Truncated S Proteins. The MERS-CoV S gene segments were synthesized by Genscript (Piscataway, NJ). The plasmid encoding residues 360-601 fused with Avi-tag was transfected into 293 Freestyle cells (Invitrogen) for transient expression and used for biopanning. Plasmids encoding residues 18-725, 18-353, 358-588, 377-588, 377-662, 726-1295 fused with the Fc fragment of IgG1 were also transfected into 293T cells (ATCC). Point mutations were generated at specific residues of the MERS-CoV RBD (residues 377-588) using QuikChange II XL site-directed mutagenesis kit (Stratagene). The RBD protein and its mutants were expressed and analyzed as described previously (21).

Generation of a large Phage-displayed IgM Fab Library, and Selection, Expression, and Purification of the RBD-specific Fabs and Conversion to IgG1s. A large phage display library was constructed by using PBMC cDNA from 40 healthy volunteers as templates for cloning the expressed antibody gene repertoire. The library was panned using MERS-CoV RBD (residues 360-601) conjugated to magnetic beads (Invitrogen). Amplified libraries of 10^{12} phage-displayed Fabs were incubated with 5, 3, 3 and 1 μg of RBD for 2 h at room temperature during

140 the first, second, third and fourth rounds of biopanning, respectively. Clones that bound to RBD
141 were identified from the third and fourth rounds of panning by using monoclonal phage ELISA.
142 The VH and VL domains of these clones were sequenced, and twelve dominant clones were
143 identified. For conversion to IgG1, the heavy and light chains of Fabs m336, m337 and m338
144 were amplified and re-cloned into the pDR12 vector (provided by D. Burton, Scripps Research
145 Institute, La Jolla, CA). Both Fabs and IgG1s were expressed and purified. Protein purity was
146 estimated as >95% by SDS-PAGE and protein concentration was measured
147 spectrophotometrically (NanoVue, GE Healthcare).

148

149 **ELISA.** The MERS-CoV RBD (residues 360-601) protein was coated on a 96-well plate
150 (Costar) at 50 ng/well in PBS overnight at 4^{o}C. For phage ELISA, phage from each round of
151 panning (polyclonal phage ELISA) or clones randomly picked from the infected TG1 cells
152 (monoclonal phage ELISA) were incubated with immobilized antigen. Bound phage were
153 detected with anti-M13-HRP polyclonal Ab (Pharmacia, Piscataway, NJ). For the soluble Fab
154 binding assay, HRP-conjugated mouse anti-FLAG tag Ab (Sigma-Aldrich) was used to detect
155 Fab binding. For the IgG1 binding assay, HRP-conjugated goat anti-human IgG Ab (Sigma-
156 Aldrich) was used for detection. For the competition ELISA, 20 nM of Fabs were incubated with
157 serially diluted IgG1s, and the mixtures were added to RBD-coated wells. After washing, bound
158 Fabs were detected by HRP-conjugated mouse anti-FLAG tag Ab (Sigma-Aldrich). For
159 inhibition of MERS-CoV RBD binding to DPP4, recombinant soluble DPP4 was coated on plate.
160 The MERS-CoV RBD (residues 377-588)-Fc fusion protein was incubated with serially diluted
161 m336, m337 or m338, and the mixtures were added to DPP4-coated wells. After washing, bound

RBD-Fc fusion protein was detected by HRP-conjugated goat anti-human IgG Ab (Sigma-Aldrich).

Surface Plasmon Resonance. Binding of Fabs and IgG1s to the RBD was assayed using a BiacoreX100 instrument. Purified RBD was diluted in 10 mM sodium acetate buffer, pH 5.0, and immobilized on a CM5 sensor chip with an amine coupling kit. The reference flow cell was treated with the amine coupling reagent without exposure to the RBD. The running buffer was HBS-EP (10 mM HEPES, pH 7.4, 150 mM NaCl, 3 mM EDTA, 0.05% surfactant P20). The chip was regenerated with 10 mM glycine pH 2.5, and 1 M NaCl. The sensorgram was analyzed with BiaEvaluation software, and data were fitted to a 1:1 binding model.

MERS-CoV Pseudovirus Neutralization Assay. MERS pseudovirus bearing MERS-CoV S protein and a defective HIV-1 genome that expresses luciferase as reporter was prepared by co-transfecting 293T cells with the plasmid pNL4-3.luc.RE (encoding Env-defective, luciferase-expressing HIV-1) and pcDNA3.1-MERS-CoV-S plasmid. To detect the inhibitory activity of mAbs on infection by MERS pseudovirus, DPP4-expressing Huh-7 cells (10^4/well in 96-well plates) were infected with MERS-CoV pseudovirus in the presence or absence of RBD-specific mAbs m336, m337 and m338 at indicated concentrations. The culture was re-fed with fresh medium 12 h post-infection and incubated for an additional 72 h. Cells were washed with PBS and lysed using lysis reagent included in a luciferase kit (Promega). Aliquots of cell lysates were transferred to 96-well flat-bottom luminometer plates (Costar), followed by addition of luciferase substrate (Promega). Relative light units were determined immediately using the Ultra 384 luminometer (Tecan USA).

185

186 **MERS-CoV Neutralization Assay.** A clinical isolate of MERS-CoV was kindly
187 provided by R. Fouchier, A. Zaki, and colleagues. The isolate was cultured in Vero cells with
188 DMEM medium at 37°C. Two or 3 days after virus inoculation, culture supernatants were
189 collected. Serial two-fold diluted mAbs m336, m337 and m338 were prepared in duplicate in a
190 96-well tissue culture plate in MEM medium supplemented with 1% FCS. An equal volume of
191 MERS-CoV working stock containing 200 $TCID_{50}$ was added, and the antibody-virus mixture
192 was incubated for 2 h at 37^{o}C. Antibody-virus mixtures were added into a 96-well microtitre
193 plate (Costar) containing equal volume of confluent Vero cells. After incubation at 37^{o}C for 3
194 days, the plate was observed for cytopathic effect.

195

196 **Molecular Modeling and Docking**. The prediction of immunoglobulin structures (PIGS)
197 server (22) was used for automated construction of the three-dimensional (3D) structures of Fv
198 regions of mAbs m336, m337 and m338, using a canonical structure based approach for CDRs,
199 L1-L3, H1 and H2, and grafting of the HCDR3s from known structures. Different criteria for
200 light/heavy chain template selection such as “Same Antibody” and “Best H and L chains” were
201 explored. The conformations of side chains were maintained as long as those residues were
202 conserved between the target and the template while side chains from other residues were
203 modeled using SCWRL 3.0 as implemented. Finally, the 3D models of mAbs from Fv m336,
204 m337 and m338 were selected without any steric clashes at the VH/VL interface. The ZDOCK
205 3.0.2 program (23) was employed to dock the mAbs onto the MERS-CoV RBD for which a
206 crystal structure is available. The docking output was filtered by selecting at least one potential
207 contacting residue on the RBD, for example D539 in RBD, and a residue from the center of the

antigen combining site of mAbs, an Arg residue in the torso region of HCDR3 of m336. The top 10 MERS-CoV RBD docked complexes among the predictions were visually scrutinized. Docked models with the most compatibility to general aspects of antibody-antigen structural features such as hydrogen bonds, salt bridges and other interactions at the interface without any highly unusual features or clashes were selected.

RESULTS

Selection of high-affinity Fabs to the MERS-CoV RBD from a very large naïve human phage displayed antibody library. To select high-affinity antibodies without additional maturation we constructed a very large (size ~ 10^{11}) phage-displayed antibody Fab library made by using B cells from the blood of 40 healthy donors. Preliminary characterization of this library indicated very high diversity demonstrated also by identification of high-affinity binders towards various viral and cancer-related antigens. This library was panned against recombinant MERS-CoV RBD developed in our laboratory (**FIG 1**). Panning resulted in significant enrichment after 3-4 rounds. Screening against the same protein led to the identification of a panel of 12 Fabs which bound with varying affinities to the RBD as demonstrated by ELISA and Biacore (**FIG 1, 2**). Three Fabs designated as m336,7,8 had the lowest concentrations of 50% binding (EC50s). Interestingly, we found that all three mAbs emerged from the common germline VH gene 1-69 (Table 1).

Generation of full-size antibodies in IgG1 format and their binding to the RBD. The Fabs m336,7,8 were selected for further characterization and converted to an IgG1 format. The mAbs bound with high (pM) avidity (K_d 9.94×10^{-11} to 8.23×10^{-10} M) to RBD as measured by

231 Biacore (**Table 1**) but the negative control IgG1, m610.27, which has the same constant domains
232 as m336,7,8 did not (**data not shown**). Their high affinity/avidity and specificity suggest
233 potential use as research reagents for exploring mechanisms of viral entry and for diagnosis of
234 MERS-CoV infections.

235

236 **Neutralization of MERS-CoV infection by RBD-specific mAbs.** The neutralization
237 activity of IgG1s m336, m337 and m338 against MERS-CoV were first evaluated by using a
238 pseudovirus system. Single-round HIV luciferase reporter viruses pseudotyped with MERS-CoV
239 S protein were tested for neutralization sensitivity against increasing concentration of mAbs. As
240 shown in **FIG 3A**, all three RBD-specific mAbs exhibited exceptionally potent
241 neutralizationactivity with 50% inhibitory concentration (IC_{50}) ranging from 0.005 to 0.017
242 μg/mL. Notably, the most potent mAb, m336, inhibited >90% MERS-CoV pseudovirus infection
243 at a concentration of 0.039 μg/mL, while the negative control IgG1 m610.27 was unable to
244 inhibit the infection (**data not shown**).

245 We next tested the neutralization activity of the mAbs with live MERS-CoV virus (**FIG**
246 **3B**). Similarly, m336 showed the most potent neutralization activity with IC_{95} of 1 μg/ml and
247 IC_{50} of 0.07 μg/ml. To our knowledge these are the first fully human mAbs known to neutralize
248 both pseudotyped and live MERS-CoV with such high potency.

249

250 **RBD-specific mAbs competed with the MERS-CoV receptor DPP4 for binding to**
251 **the virus**. We used several S1 fragments, a soluble DPP4 (sDPP4), alanine mutagenesis and

molecular modeling to define the epitopes of the antibodies and elucidate the mechanism of neutralization.

MERS-CoV S fragments S18-725, S18-353, S358-588, S377-588, S377-662, S726-1295 fused with the Fc fragment of IgG1 were generated (**FIG 4A**). As shown in **FIG 4B-D**, m336, m337 and m338 bound potently to fragments containing the RBD (S18-725-Fc, S358-588-Fc, S377-588-Fc, and S377-662-Fc), but not to fragments lacking the RBD (S726-1295-Fc and S18-353-Fc). These data confirm that the binding sites of these mAbs are within the MERS-CoV RBD and, specifically, in the residues 377-588 region.

We next evaluated whether mAbs m336, m337 and m338 were capable of inhibiting the binding of MERS-CoV RBD to the receptor DPP4. We first confirmed that the three mAbs competed with each other for binding to the MERS-CoV S1 glycoprotein (**FIG 5A**). Furthermore, as shown in **FIG 5B**, all the IgG1s potently inhibited the binding of RBD to the soluble DPP4 receptor. Consistent with the neutralization results, m336 IgG1 was slightly more potent that m337 and m338 in blocking the binding of RBD to the receptor. The 50% inhibitory concentration (IC_{50}) of m336, m337 and m338 were 0.034, 0.044 and 0.041 μg/mL, respectively. Taken together, these results suggest that the mAbs neutralize the virus by competing with the receptor for binding to the RBD and have overlapping epitopes.

To further localize the mAbs epitopes, a panel of RBD alanine-scanning mutants was developed guided by structural information available for the RBD. Binding of mAbs to the mutants were measured by ELISA (**FIG 6**). Binding of m336 to RBD with mutated residues L506A, D510A, E536A, D539A, W553A, and V555A was considerably reduced, as was binding of m337 to mutants L506A, D510A, E553A, and V555A, and m338 to mutants D510A and W553A. These results indicate that the three RBD-specific mAbs possess overlapping but

distinct epitopes. In addition, the most potent mAb, m336, uniquely lost binding to the E536/D539 mutant, indicating that these RBD residues are crucial for interactions with m336 and could be part of a promising template for the development of vaccine immunogens. In contrast, residues D510 and W553 appear to be important for RBD binding to all three mAbs.

Molecular modeling of RBD-specific mAbs and docking with the MERS-CoV RBD. We used the mutagenesis data and the RBD crystal structure (24, 25) to build docking models (**FIG 7**). Both the Fv regions of light and heavy chains of mAbs, m336, m337 and m338, were modeled using the best matches with highest sequence identities of known templates from different structures. All the CDRs except the HCDR3 were modeled based on canonical conformations defined for those particular canonical structure classes. Although there are such no canonical structures for HCDR3, HCDR3 of RBD-specific mAbs were grafted from structurally known antibodies with the same HCDR3 lengths. This combined approach resulted in the 3D models of RBD-specific mAbs as shown in **FIG 7A-C**. In the case of m336, the HCDR3 template (PDB code: 3EYF) also had a centrally located cysteine residues that form disulfide bond which could be used to stabilize the conformation of HCDR3 with a length of 18 amino acids in m336. The other two mAbs, m337 and m338, had multiple tyrosine residues within the HCDR3s that might be of structural significance as well as active antigen recognition sites. For docking simulations, at least one of the HCDR3 residues well solvent-exposed and located at the middle of the antigen combining site was considered as a contacting residue in m336. Similarly, one of the most prominent residues identified from the site-directed mutagenesis experiment as well as located at the RBD surface was considered as a contacting residue in the MERS-CoV RBD. The similar docking constraints for m337 and m338 helped in

selecting the docked complexes that might predict potential binding residues at the interface of MERS-CoV RBD-mAbs complexes (**Table 2**). The known crystal structure of MERS-CoV RBD bound to DPP4 (24, 25) was superimposed to each of three mAbs by aligning the RDB region as shown in **FIG 7D**. These results indicated a possible dominant role of the heavy chain in the mAb paratopes and putative epitope forming RBD residues (**Table 2)**, showing the overlap between the mAb epitopes and the receptor binding site (**FIG 7D**) and molecular details of the mAb-RBD interactions which may have implications for design of vaccine immunogens and small molecule drugs.

DISCUSSION

The major results of this study are the identification and characterization of novel human mAbs against the recently emerged MERS-CoV which bind to the MERS-CoV RBD with very high affinity (pM) and inhibit infection with exceptional potency. We attempted to test the antibody inhibitory activity in mice but the level of virus was very low likely due to the inefficient or lacking virus entry mediated by the mouse DPP4 (26). Therefore, a better model should be used to evaluate the antibody potency in vivo. Interestingly, the IGHV genes of m336,7,8 originated from IGVH1-69. It is noted that the IGHV1-69 gene is also preferentially utilized by other anti-viral antibodies including HIV-1 (27), influenza (28) and hepatitis C virus (29).

We found that that the three mAbs compete with each other and with the receptor DPP4 for binding to the S glycoprotein, suggesting a competitive mechanism of virus neutralization. Several other mAbs against emerging viruses including SARS-CoV and henipaviruses have been previously identified which exhibited high potency in vitro and in animal models of infection (18-20), and used in humans exposed to Hendra virus (30). Because they competed with the

receptors and some bound to the receptor binding site (RBS) they were highly cross-reactive. For example, m102.4 inhibited both Hendra and Nipah viruses which use the same receptor for entry into cells. Therefore, one can expect that the newly identified antibodies will be effective against many if not all MERS-CoV isolates. We analyzed the sequences of a total of 11 MERS-CoV strains, and found that overall their sequences are highly conserved. Only 5 residues out of the MERS-CoV S1 glycoprotein (725 residues in length) and only one in the RBD region contained any variation at all. In addition, one could expect that emergence of resistant viruses if any will exert a toll on the virus fitness because the mutant virus may have lower affinity for the receptor. However, further experiments to test the m336 against different isolates as well against emergence of resistant mutants are needed to confirm this possibility.

These newly identified mAbs are promising candidate therapeutics against the MERS-CoV because of their exceptionally high neutralization activity which could accelerate their further development for prophylaxis and therapy of MERS-CoV infection in humans. We also expect their uses as a reagent to facilitate the development of highly immunogenic vaccines against MERS-CoV. We have found that significant neutralizing antibody responses could be induced by immunizing BALB/c mice with purified MERS-CoV RBD protein (31). Taken together, these results suggesting that RBD, especially the epitopes that targeted by these exceptionally potent RBD-specific mAbs, has great potential to be developed as a highly effective MERS-CoV vaccine. Additionally, the rapid (several weeks) identification of three potent mAbs described in this work suggests a possibility to use the large non-immune antibody library and related methodology for quick response to public threat resulting from emerging SARS-like or MERS-like coronaviruses, which are highly likely to continue to emerge and pose a serious threat to human health in the near future. MERS CoV continues to cause major illness

and even has killed a number of people in close contacts of patients as have been reported (2, 32). These mAbs may help treat patients in similar situations and can be life-saving intervention for those who have been infected and at the risk of MERS CoV infections.

ACKNOWLEDGEMENTS

We thank Dr. Fang Li in University of Minnesota for useful discussions. This work was supported by the Intramural Research Program of the NIH, National Cancer Institute, Center for Cancer Research, and by Federal funds from the NIH, National Cancer Institute, under Contract Nos. N01-CO-12400 and HHSN261200800001E.

REFERENCES

1. **Zaki AM, van Boheemen S, Bestebroer TM, Osterhaus AD, Fouchier RA.** 2012. Isolation of a novel coronavirus from a man with pneumonia in Saudi Arabia. N Engl J Med **367:**1814-1820.
2. **Assiri A, McGeer A, Perl TM, Price CS, Al Rabeeah AA, Cummings DA, Alabdullatif ZN, Assad M, Almulhim A, Makhdoom H, Madani H, Alhakeem R, Al-Tawfiq JA, Cotten M, Watson SJ, Kellam P, Zumla AI, Memish ZA.** 2013. Hospital outbreak of Middle East respiratory syndrome coronavirus. N Engl J Med **369:**407-416.
3. **Cotten M, Watson SJ, Kellam P, Al-Rabeeah AA, Makhdoom HQ, Assiri A, Al-Tawfiq JA, Alhakeem RF, Madani H, AlRabiah FA, Al Hajjar S, Al-nassir WN, Albarrak A, Flemban H, Balkhy HH, Alsubaie S, Palser AL, Gall A, Bashford-Rogers R, Rambaut A, Zumla AI, Memish ZA.** 2013. Transmission and evolution of the Middle East respiratory syndrome coronavirus in Saudi Arabia: a descriptive genomic study. Lancet **382:**1993-2002.
4. **Ithete NL, Stoffberg S, Corman VM, Cottontail VM, Richards LR, Schoeman MC, Drosten C, Drexler JF, Preiser W.** 2013. Close relative of human Middle East respiratory syndrome coronavirus in bat, South Africa. Emerging infectious diseases **19:**1697-1699.
5. **Haagmans BL, Al Dhahiry SH, Reusken CB, Raj VS, Galiano M, Myers R, Godeke GJ, Jonges M, Farag E, Diab A, Ghobashy H, Alhajri F, Al-Thani M, Al-Marri SA, Al Romaihi HE, Al Khal A, Bermingham A, Osterhaus AD, Alhajri MM, Koopmans MP.** 2014. Middle East respiratory syndrome coronavirus in dromedary camels: an outbreak investigation. The Lancet infectious diseases **14:**140-145.

6. **Graham RL, Donaldson EF, Baric RS.** 2013. A decade after SARS: strategies for controlling emerging coronaviruses. Nature reviews. Microbiology **11:**836-848.
7. **Falzarano D, de Wit E, Rasmussen AL, Feldmann F, Okumura A, Scott DP, Brining D, Bushmaker T, Martellaro C, Baseler L, Benecke AG, Katze MG, Munster VJ, Feldmann H.** 2013. Treatment with interferon-alpha2b and ribavirin improves outcome in MERS-CoV-infected rhesus macaques. Nat Med **19:**1313-1317.
8. **Dimitrov DS.** 2012. Therapeutic proteins. Methods Mol Biol **899:**1-26.
9. **Schrama D, Reisfeld RA, Becker JC.** 2006. Antibody targeted drugs as cancer therapeutics. Nat Rev Drug Discov **5:**147-159.
10. **Casadevall A, Dadachova E, Pirofski L.** 2004. Passive antibody therapy for infectious diseases. Nature Reviews Microbiology **2:**695-703.
11. **Carter PJ.** 2006. Potent antibody therapeutics by design. Nature Reviews Immunology **6:**343-357.
12. **Scott LJ, Lamb HM.** 1999. Palivizumab. Drugs **58:**305-311; discussion 312-303.
13. **Prabakaran P, Zhu Z, Xiao X, Biragyn A, Dimitrov AS, Broder CC, Dimitrov DS.** 2009. Potent human monoclonal antibodies against SARS CoV, Nipah and Hendra viruses. Expert Opin Biol Ther **9:**355-368.
14. **Marasco WA, Sui J.** 2007. The growth and potential of human antiviral monoclonal antibody therapeutics. Nature biotechnology **25:**1421-1434.
15. **Kwong PD, Mascola JR.** 2012. Human antibodies that neutralize HIV-1: identification, structures, and B cell ontogenies. Immunity **37:**412-425.
16. **Zhu Z, Dimitrov AS, Bossart KN, Crameri G, Bishop KA, Choudhry V, Mungall BA, Feng YR, Choudhary A, Zhang MY, Feng Y, Wang LF, Xiao X, Eaton BT, Broder CC, Dimitrov DS.** 2006. Potent neutralization of Hendra and Nipah viruses by human monoclonal antibodies. J Virol **80:**891-899.
17. **Bossart KN, Tachedjian M, McEachern JA, Crameri G, Zhu Z, Dimitrov DS, Broder CC, Wang LF.** 2008. Functional studies of host-specific ephrin-B ligands as Henipavirus receptors. Virology **372:**357-371.
18. **Bossart KN, Zhu Z, Middleton D, Klippel J, Crameri G, Bingham J, McEachern JA, Green D, Hancock TJ, Chan YP, Hickey AC, Dimitrov DS, Wang LF, Broder CC.** 2009. A neutralizing human monoclonal antibody protects against lethal disease in a new ferret model of acute nipah virus infection. PLoS Pathog **5:**e1000642.
19. **Bossart KN, Geisbert TW, Feldmann H, Zhu Z, Feldmann F, Geisbert JB, Yan L, Feng YR, Brining D, Scott D, Wang Y, Dimitrov AS, Callison J, Chan YP, Hickey AC, Dimitrov DS, Broder CC, Rockx B.** 2011. A neutralizing human monoclonal antibody protects african green monkeys from hendra virus challenge. Sci Transl Med **3:**105ra103.
20. **Zhu ZY, Chakraborti S, He Y, Roberts A, Sheahan T, Xiao XD, Hensley LE, Prabakaran P, Rockx B, Sidorov IA, Corti D, Vogel L, Feng Y, Kim JO, Wang LF, Baric R, Lanzavecchia A, Curtis KM, Nabel GJ, Subbarao K, Jiang S, Dimitrov DS.** 2007. Potent cross-reactive neutralization of SARS coronavirus isolates by human monoclonal antibodies. Proceedings of the National Academy of Sciences of the United States of America **104:**12123-12128.
21. **Du L, Kou Z, Ma C, Tao X, Wang L, Zhao G, Chen Y, Yu F, Tseng CT, Zhou Y, Jiang S.** 2013. A Truncated Receptor-Binding Domain of MERS-CoV Spike Protein Potently Inhibits MERS-CoV Infection and Induces Strong Neutralizing Antibody

Responses: Implication for Developing Therapeutics and Vaccines. PLoS ONE **8:**e81587.

22. **Marcatili P, Rosi A, Tramontano A.** 2008. PIGS: automatic prediction of antibody structures. Bioinformatics **24:**1953-1954.
23. **Chen R, Li L, Weng Z.** 2003. ZDOCK: an initial-stage protein-docking algorithm. Proteins **52:**80-87.
24. **Lu G, Hu Y, Wang Q, Qi J, Gao F, Li Y, Zhang Y, Zhang W, Yuan Y, Bao J, Zhang B, Shi Y, Yan J, Gao GF.** 2013. Molecular basis of binding between novel human coronavirus MERS-CoV and its receptor CD26. Nature **500:**227-231.
25. **Wang N, Shi X, Jiang L, Zhang S, Wang D, Tong P, Guo D, Fu L, Cui Y, Liu X, Arledge KC, Chen YH, Zhang L, Wang X.** 2013. Structure of MERS-CoV spike receptor-binding domain complexed with human receptor DPP4. Cell research **23:**986-993.
26. **Devitt E.** 2013. Lack of small animal model hinders MERS coronavirus research. Nat Med **19:**952.
27. **Prabakaran P, Zhu Z, Chen W, Gong R, Feng Y, Streaker E, Dimitrov DS.** 2012. Origin, diversity, and maturation of human antiviral antibodies analyzed by high-throughput sequencing. Frontiers in microbiology **3:**277.
28. **Ohshima N, Iba Y, Kubota-Koketsu R, Asano Y, Okuno Y, Kurosawa Y.** 2011. Naturally occurring antibodies in humans can neutralize a variety of influenza virus strains, including H3, H1, H2, and H5. J Virol **85:**11048-11057.
29. **Chan CH, Hadlock KG, Foung SK, Levy S.** 2001. V(H)1-69 gene is preferentially used by hepatitis C virus-associated B cell lymphomas and by normal B cells responding to the E2 viral antigen. Blood **97:**1023-1026.
30. **Zhu Z, Prabakaran P, Chen W, Broder CC, Gong R, Dimitrov DS.** 2013. Human monoclonal antibodies as candidate therapeutics against emerging viruses and HIV-1. Virologica Sinica **28:**71-80.
31. **Du L, Zhao G, Kou Z, Ma C, Sun S, Poon VK, Lu L, Wang L, Debnath AK, Zheng BJ, Zhou Y, Jiang S.** 2013. Identification of a receptor-binding domain in the S protein of the novel human coronavirus Middle East respiratory syndrome coronavirus as an essential target for vaccine development. J Virol **87:**9939-9942.
32. **Memish ZA, Zumla AI, Al-Hakeem RF, Al-Rabeeah AA, Stephens GM.** 2013. Family cluster of Middle East respiratory syndrome coronavirus infections. N Engl J Med **368:**2487-2494.

FIGURE LEGENDS

FIG 1 (A) Schematic structure of MERS-CoV S subunit and RBD(360-601)-avi tag. SP: signal peptide. RBD(360-601)-avi tag was constructed by fusing MERS-CoV residues 360-601 of S1 with Avi-tag. (B) Polyclonal phage ELISA showing the binding of the first to fourth rounds of phage to RBD. Bound phage were detected with anti-M13-HRP polyclonal Ab. (C) Binding of m331 to m342 Fabs to RBD. HRP-conjugated mouse anti-FLAG tag Ab was used to detect Fab binding.

FIG 2 Binding of Fabs m336, m337 and m338 to MERS-CoV RBD measured by BIAcore. RBD was immobilized on a CM5 chip. The analytes consisted of serial dilution of proteins between 0.5 μM and 0.8 nM. The chip was regenerated with 10 mM glycine pH 2.5, 1 M NaCl.

FIG 3 Potent in vitro neutralization of MERS-CoV by RBD-specific mAbs. (A) Neutralization of viruses pseudotyped with the MERS-CoV S glycoprotein. Pseudotyped virus was incubated with IgG1s before infection of DPP4-expressing Huh-7 cells. Luciferase activities were measured and percent neutralization was calculated. (B). Neutralization of live virus. MERS-CoV was incubated with IgG1s before infection of Vero cells. Cytopathic effects were measured and percent neutralization was calculated.

FIG 4 Binding of Fabs to different MERS-CoV S segments. (A) Schematic structure of MERS-CoV S subunits S18-725, S18-353, S358-588, S377-588, S377-662, S726-1295 fused with the Fc fragment of IgG1. m336 (B), m337 (C) and m338 (D) bound to S18-725-Fc, S358-588-Fc, S377-588-Fc, S377-662-Fc, but not to S726-1295-Fc, S18-353-Fc.

FIG 5 mAbs competed with the MERS-CoV receptor DPP4 for binding to RBD. (A) m336,7,8 competed with each other for binding to the MERS-CoV RBD. Fabs were incubated with serially diluted IgG1s, and the mixtures were added to RBD-coated wells. After washing, bound Fabs were detected by HRP-conjugated mouse anti-FLAG tag Ab. (B) The MERS-CoV RBD-Fc fusion protein was incubated with serially diluted IgG1s, and the mixtures were added to DPP4-coated wells. After washing, bound RBD-Fc fusion protein was detected by HRP-conjugated goat anti-human IgG Ab.

FIG 6 Binding of Fab m336 (A), m337 (B) and m338 (C) to different MERS-CoV RBD mutants.

FIG 7 Docked complexes of MERS-CoV RBD with mAbs (A) m336, (B) m337 and (C) m338. (D) Superposition of the docked complexes of RBD-m336,7,8 and the crystal structure of the RBD-DPP4 complex.

Table 1 Gene usage and binding kinetics features of MERS-CoV RBD-specific Fabs and IgG1s.

	m336	m337	m338
Gene usage			
V_H	1-69*06	1-69*06, 08 or 14	1-69*09
D_H	2-2*03	3-22*01	3-22*01
J_H	J3*02	J3*02	J3*02
V_L[†]	1-17*01	2-28*01, 2D-28*01	3-11*01
J_L	4*01	4*01	1*01
Fabs			
k_{on} (Ms^{-1})	4.50×10^{6}	4.49×10^{4}	3.68×10^{4}
k_{off} (s^{-1})	1.92×10^{-2}	4.19×10^{-4}	5.54×10^{-4}
K_d (M)	4.27×10^{-9}	9.34×10^{-9}	1.51×10^{-8}
IgG1s			
k_{on} ($M^{-1}s^{-1}$)	1.66×10^{6}	1.87×10^{5}	3.55×10^{5}
k_{off} (s^{-1})	1.65×10^{-4}	1.54×10^{-4}	1.98×10^{-4}
K_d (M)	9.94×10^{-11}	8.23×10^{-10}	5.59×10^{-10}

[†] All three are kappa light chains

Table 2 Putative binding residues predicted from the docked complexes of MERS-CoV RBD-m336,7 8. H and HS indicate possible hydrogen bonds and hydrogen bonds/salt bridges across the molecular interface.

MERS-CoV RBD	**mAb m336**	**MERS-CoV RBD**	**mAb m337**	**MERS-CoV RBD**	**mAb m338**
	(VH)		**(VH)**		**(VH)**
Lys493	Thr28	Phe467	Ser31H	Leu495	Ser31
Leu495H	Ser30	Asn501	Tyr32	Ile529	Arg50
Lys496	Tyr32	Lys502H	Ile52H	Ser532H	Ile52
Y499	Tyr101	Leu506	Phe55	Pro531	Leu55
Asn501	Ser104	Asp510H	Thr57H	Thr533	Ile57
Thr533	Thr105	Arg511H	Asn59	Trp535H	Asn59
Trp535	Arg109HS	Glu513S	Gln65H	Glu536H	Asp102
Glu536HS	Ala111H	Pro531	Leu100	Asp539	Ser104H
ASP537	Asp113H	Trp535	Asp105	Tyr540	Tyr106
Asp539HS	Ile114	Glu536HS	Tyr110	Tyr541	Tyr107
Tyr540	**(VL)**	Asp539H	**(VL)**	Arg542H	Arg108
Arg542	Tyr49	Tyr540H	Gln27	Lys543	**(VL)**
Val561	Gln55	Arg542HS	His31S	Gln544H	Gln27
Met563	Ser56	Lys543	Leu97	Trp553	His31S
Glu565		Gln544H	Gln98		Leu97
		Trp553	Thr99		Gln98
					Thr99

A

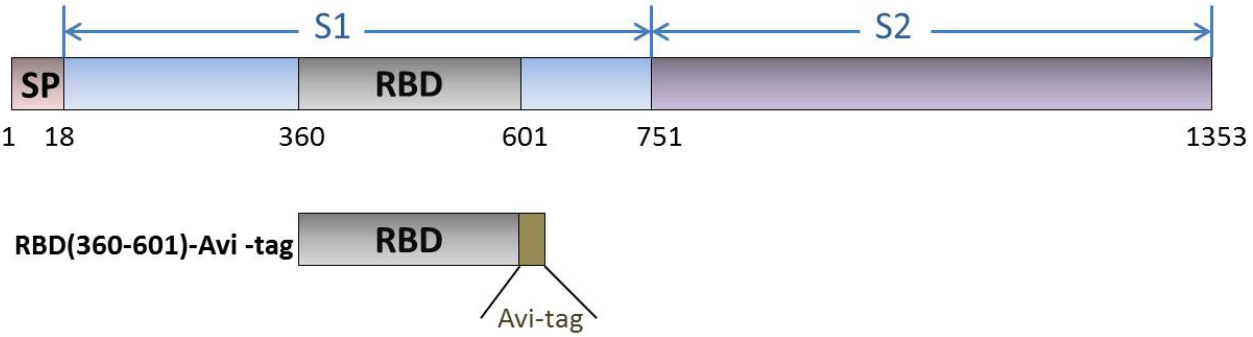

B

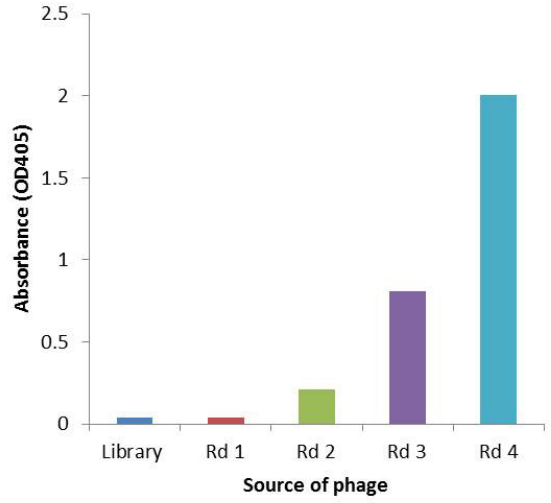

C